RESEARCH ARTICLE

Finely Tuned γ Tracks Medication Cycles in Parkinson's Disease: An Ambulatory Brain-Sense Study

Aaron Colombo, MSc,[1,2] Elena Bernasconi, MSc,[1,3] Laura Alva, MD,[1] Mario Sousa, MD,[1] Ines Debove, MD,[1]
Andreas Nowacki, MD,[4] Camille Serquet, MSc,[1] Katrin Petermann, MSc,[1] T.A. Khoa Nguyen, PhD,[2,4]
Andreia D. Magalhães, MD, PhD,[1] Lenard Lachenmayer, MD,[1] Julia Waskönig, MD,[1] Tobias Nef, PhD,[1,2]
Michael Schuepbach, MD,[5] Claudio Pollo, MD,[4] Paul Krack, MD, PhD,[1] Alberto Averna, PhD,[1] and
Gerd Tinkhauser, MD, PhD[1*]

ABSTRACT: Background: Novel commercial brain-sense neurostimulators enable us to contextualize brain activity with symptom and medication states in real-life ambulatory settings in Parkinson's disease (PD). Although various candidate biomarkers have been proposed for adaptive deep brain stimulation (DBS), a comprehensive comparison of their ambulatory profiles is lacking.
Objectives: To systematically compare the ambulatory neurophysiological dynamics and clinical properties of three candidate biomarkers—low-frequency, beta (β), and finely tuned γ (FTG) activity.
Methods: We investigated 14 PD patients implanted with the Medtronic Percept PC, who underwent up to two 4-week ambulatory multimodal recording periods on their regular medication and stimulation. Subthalamic nucleus local field potentials (LFPs) of low-frequency, β, and FTG activity were recorded. Additionally, objective motor symptom states, physical activity and heart rate using wearables, as well as medication-intake times, sleep-awake times, and subjective symptom states using diaries were co-registered. LFP dynamics were also compared to high-resolution in-hospital recordings under *off/on* dopaminergic medication and stimulation conditions.

Results: FTG reliably indexed *off* to *on* medication states in the ambulatory setting at the group and individual levels, and these spectral dynamics could be anticipated by high-resolution in-hospital recordings. Both FTG and low-frequency correlated with wearable-based dyskinesia scores, whereas diary-based dyskinesia events were only linked to FTG. Importantly, FTG indicated *on*-medication states regardless of the presence of dyskinesia and despite potential motion and heart rate artifacts. The 24-hour profile revealed large circadian power shifts that may overdrive medication-intake dynamics.
Conclusion: Despite the limitations of low-temporal resolution recordings, this work provides valuable insights into the real-life dynamics of biomarkers. Specifically, it highlights the utility of FTG as a primary and reliable indicator of medication states for adaptive DBS. © 2025 The Author(s). *Movement Disorders* published by Wiley Periodicals LLC on behalf of International Parkinson and Movement Disorder Society.

Key Words: brain-sense; Parkinson's disease; closed-loop, adaptive deep brain stimulation; biomarkers; home recording

---

[1]Department of Neurology, Bern University Hospital and University of Bern, Bern, Switzerland; [2]ARTORG Center for Biomedical Engineering Research, University of Bern, Bern, Switzerland; [3]Graduate School of Cellular and Biomedical Sciences (GCB), University of Bern, Bern, Switzerland; [4]Department of Neurosurgery, Bern University Hospital and University of Bern, Bern, Switzerland; [5]Institute of Neurology, Konolfingen, Switzerland

***Correspondence to:** Dr. Gerd Tinkhauser, Department of Neurology, Bern University Hospital, Freiburgstrasse, 3010 Bern, Switzerland; E-mail: gerd.tinkhauser@insel.ch

Aaron Colombo and Elena Bernasconi have equal contribution to first authorship. Alberto Averna and Gerd Tinkhauser have equal contribution to last authoship.

Adaptive closed-loop DBS (aDBS) is advancing into clinical practice[1-6] and requires a thorough understanding of strengths and limitations of neurophysiological symptom biomarkers in patients' daily lives.[4,7,8]

Over the past decades, neurophysiological basal ganglia signals in patients with Parkinson's disease (PD) have almost exclusively been studied under constrained in-hospital conditions.[9-17] Only recent advancements in neurostimulator technology allow us to track brain activity in real-life settings over longer time periods to validate existing and discover novel biomarkers.[8,18,19] Currently, β activity (13–30 Hz) is the best characterized neurophysiological biomarker for PD, associated with akinetic symptoms and suppressed by both medication and stimulation.[9,12,20,21] Most aDBS studies have successfully used β activity as a feedback signal.[1,2,22,23] Finely tuned γ (FTG) or narrowband γ activity is emerging as another promising neurophysiological biomarker in PD, characterized by two distinct spectral phenomena: levodopa-induced FTG typically appearing at 70–90 Hz and stimulation-entrained FTG that emerges at half the stimulation frequency (e.g., 62.5 Hz when stimulating at 125 Hz). Both have been linked to dyskinesia. Importantly, stimulation-entrained FTG can also be further increased by dopaminergic medication.[24-30] FTG picked up from the cortex has already been shown to be an effective feedback signal for adjusting DBS in real time,[31] whereas subcortical FTG is less well understood.[32] Moreover, although discussed less, also elevated low-frequency activity (5–12 Hz) has been linked to high dopaminergic states and dyskinesia.[10,11,33] It can also inform about tremor,[34-38] bradykinesia,[39,40] neuropsychiatric symptoms,[41-44] and sleep states[25,45,46] and may be useful as a biomarker for aDBS.[45,47-49]

This study systematically compares the neurophysiological dynamics and clinical properties of three candidate biomarkers—low-frequency, β, and FTG activity over multiple weeks of ambulatory recordings in PD patients implanted with commercial, sensing-enabled neurostimulators. Using a multimodal approach with wearables, symptom logs, and medication tracking, we evaluated these biomarkers in relation to dopaminergic medication cycles, motor fluctuations, and circadian rhythms, while accounting for confounding factors such as cardiac and motion artifacts. Ambulatory data were also compared to high-resolution in-hospital assessments. The goal is to provide comprehensive insights into different biomarkers and their role for sensing-guided treatment strategies.

Methods

Patients

Fourteen PD patients with STN-DBS, 12 men and 2 women, implanted with the Percept PC (Medtronic, Minneapolis, MN, USA) and directional leads at Bern University Hospital were included (Table 1). The average age of the participants at the time of the assessment was 60 years (range: 38–70), with a mean disease duration of 11 years (range: 6–17). The preoperative Movement Disorders Society—Unified Parkinson's Disease Rating Scale Part 3 (MDS-UPDRS-III) score off-medication and OFF-stimulation was on average 44 (range: 19–64). The implantation procedure is described in the supplementary material. All patients provided written informed consent (Swiss ethics number: 2020-00200).

Experimental Setup

The first assessment has been conducted for an average of 10 months (range: 3–20) after surgery. Ambulatory recordings were performed on chronic stimulation and under regular dopaminergic medication over periods of four consecutive weeks using the Percept BrainSense timeline feature that allows tracking power averages of one preselected frequency bin ±2.5 Hz every 10 minutes. Three candidate biomarkers including low-frequency (5–12 Hz), β (13–30 Hz), and FTG (62.5 Hz) activity were investigated (Fig. 1A). These were defined separately for the left and right subthalamic nucleus (STN) based on visual inspection of the resting state power spectra in the stimulation OFF state prior to the setup of the long-term recording (details, supplementary material). First, the most prominent β peak in the range of 13–30 Hz of either the left or right STN was selected and defined as biomarker 1. For the other hemisphere (biomarker 2), we either selected a peak in the low-frequency range between 7.81 and 12 Hz or the FTG frequency corresponding to half the stimulation frequency (62.5 Hz) (Fig. 1B). Participants were asked to participate in a second 4-week recording period (average 9 month interval between recording periods), in which the STN with biomarker 2 was switched to either the FTG or low-frequency activity, respectively, whereas biomarker 1 remained unchanged. Stimulation setting and medication schedule within the same 4-week recording session remained unchanged (Table 1). One patient (PD20) had to self-adjust the stimulation during the recording period by 0.3 mA for clinical reasons. Figure S1 illustrates the position of the active stimulation contacts in the STN. In addition, most patients underwent independent in-hospital high-resolution recordings during the four *off/on* dopaminergic medication and stimulation combinations using the BrainSense streaming mode (details, supplementary). A sub-analysis of motion-related LFP modulation was included from a separate protocol (details, supplementary).

TABLE 1 Participants' and recordings' characteristics

PID	Sex	Age [y]	Pre-Op UPDRS off/on	Site of IPG	RID	Disease duration [y]	Start after surgery [m]	Duration [d]	Stimulation Level (contacts)	Parameters A/PW/Fs [mA]/[μs]/[Hz]	Recording level (contacts)	Frequencies (biomarker) [Hz]	LEDD [mg]
PD01	M	38	53/23	Chest Le	R01	7	3	29	Le: C+L2.5(1,2,3,4,5,6)- Ri: C+L2.5(9,10,11,12,13,14)-	Le: 1.0/60/125 Ri: 0.9/60/125	Le: L1(0)L4(7) Ri: L1(8)L4(15)	Le: 8.79 (LF) Ri: 16.60 (B)	730
					R19	8	17	29	Le: C+L2.5(1,2,3,4,5,6)- Ri: C+L2.5(9,10,11,12,13,14)-	Le: 1.4/60/125 Ri: 1.4/60/125	Le: L1(0)L4(7) Ri: L1(8)L4(15)	Le: 62.50 (FTG) Ri: 16.60 (B)	500
PD02	M	63	59/18	Chest Le	R02	12	15	36	Le: C+L3(4,5,6)- Ri: C+L3(12,13,14)-	Le: 3.5/60/125 Ri: 3.5/60/125	Le: L2(1,2,3)L4(7) Ri: L2(9,10,11)L4(15)	L: 13.67 (B) Ri: 7.81 (LF)	950
					R14	13	27	30	Le: C+L3(4,5,6)- Ri: C+L3(12,13,14)-	Le: 3.5/60/125 Ri: 3.5/60/125	Le: L2(1,2,3)L4(7) Ri: L2(9,10,11)L4(15)	Le: 13.67 (B) Ri: 62.50 (FTG)	990
PD03	M	68	24/16	Chest Le	R03	6	5	28	Le: C+L3(4,5,6)- Ri: C+L3(12,13,14)-	L: 2.3/60/125 Ri: 1.7/60/125	Le: L2(1,2,3)L4(7) Ri: L2(9,10,11)L4(15)	Le: 7.81 (LF) Ri: 19.53 (B)	710
					R13	7	14	27	Le: C+L3(4,5,6)- Ri: C+L3(12,13,14)-	Le: 2.7/60/125 Ri: 1.9/60/125	Le: L2(1,2,3)L4(7) Ri: L2(9,10,11)L4(15)	Le: 62.50 (FTG) Ri: 19.53 (B)	560
PD04	M	62	55/21	Chest Le	R04	17	14	28	Le: C+L3(4,5,6)- Ri: C+L3(12,13,14)-	Le: 2.4/60/125 Ri: 1.8/60/125	Le: L2(1,2,3)L4(7) Ri: L2(9,10,11)L4(15)	Le: 7.81 (LF) Ri: 16.60 (B)	630
					R20	18	26	35	Le: C+L3(4,5,6)- Ri: C+L3(12,13,14)-	Le: 2.4/60/125 Ri: 1.8/60/125	Le: L2(1,2,3)L4(7) Ri: L2(9,10,11)L4(15)	Le: 62.50 (FTG) Ri: 16.60 (B)	510
PD05	M	58	28/13	Chest Ri	R05	11	7	32	Le: C+L3(4,5,6)- Ri: C+L3(12,13,14)-	Le: 3.0/60/125 Ri: 3.2/60/125	Le: L2(1,2,3)L4(7) Ri: L2(9,10,11)L4(15)	Le: 7.81 (LF) Ri: 13.67 (B)	790
PD06	M	48	42/22	Chest Ri	R06	8	5	43	Le: C+L3(4,5,6)- Ri: C+L3(12,13,14)-	Le: 2.6/60/125 Ri: 2.0/60/125	Le: L2(1,2,3)L4(7) Ri: L2(9,10,11)L4(15)	Le: 17.58 (B) Ri: 8.79 (LF)	530
					R12	9	12	27	Le: C+L3(4,5,6)- Ri: C+L3(12,13,14)-	Le: 3.3/40/125 Ri: 2.0/60/125	Le: L2(1,2,3)L4(7) Ri: L2(9,10,11)L4(15)	Le: 17.58 (B) Ri:62.50 (FTG)	530
PD07	F	51	52/22	Chest Le	R07	9	20	34	Le: C+ L3(4,5,6)- Ri: C+L3(12,13,14)-	Le: 2.5/60/125 Ri: 3.1/60/125	Le: L2(1,2,3)L4 (7) Ri: L2(9,10,11)L4(15)	Le: 20.51 (B) Ri: 7.81 (LF)	390
					R15	10	26	33	Le: C+L3(4,5,6)- Ri: C+L3(12,13,14)-	Le: 2.4/60/125 Ri: 3.2/60/125	Le: L2(1,2,3)L4(7) Ri: L2(9,10,11)L4(15)	Le: 20.51 (B) Ri: 62.50 (FTG)	390
PD08	M	62	59/5	Chest Ri	R08	14	20	28	Le: C+L3(4,5,6)- Ri: C+L3(12,13,14)-	Le: 2.0/60/125 Ri: 2.0/60/125	Le: L2(1,2,3)L4(7) Ri: L2(9,10,11)L4(15)	Le: 24.41 (B) R: 7.81 (LF)	370
					R18	15	26	28	Le: C+L3(4,5,6)-	Le: 2.1/60/125	Le: L2(1,2,3)L4(7)	Le: 24.41 (B)	360

(Continues)

TABLE 1 *Continued*

	Demographic data					Assessment information				Stimulation configuration		Sensing configuration		Medication
PID	Sex	Age [y]	Pre-Op UPDRS *off/on*	Site of IPG	RID	Disease duration [y]	Start after surgery [m]	Duration [d]	Stimulation Level (contacts)	Parameters A/PW/Fs [mA]/[μs]/[Hz]	Recording level (contacts)	Frequencies (biomarker) [Hz]	LEDD [mg]
									Ri: C+L3(12,13,14)-	Ri: 2.1/60/125	Ri: L2(9,10,11)L4 (15)	Ri: 62.50 (FTG)	
PD09	M	58	46/32	Chest Le	R09	17	12	28	Le: C+L3(4,5,6)- Ri: C+L3(12,13,14)-	Le: 1.6/60/125 Ri: 2.7/60/125	Le: L2(1,2,3)L4(7) Ri: L2(9,10,11)L4(15)	Le: 20.51 (B) Ri: 7.81 (LF)	820
PD10	M	57	47/19	Chest Ri	R10	13	8	35	Le: C+L3(4,5,6)- Ri: C+L3(12,13,14)-	Le: 2.4/60/125 Ri: 2.4/60/125	Le: L2(1,2,3)L4(7) Ri: L2(9,10,11)L4(15)	Le: 27.34 (B) Ri: 7.81 (LF)	440
PD11	M	63	40/11	Chest Le	R16	13	12	31	Le: C+L2.5(1,2,3,4,5,6)- Ri: C + L2.5(9,10,11,12,13,14)-	Le: 1.2/60/125 R: 1.2/60/125	Le: L1(0)L4(7) Ri: L1(8)L4(15)	L: 17.58 (B) Ri: 8.79 (LF)	800
					R11	12	9	29	Le: C+L2.5(1,2,3,4,5,6)- Ri: C+L2.5(9,10,11,12,13,14)-	Le: 1.2/60/125 Ri: 1.2/60/125	Le: L1(0)L4(7) Ri: L1(8)L4(15)	Le: 17.58 (B) Ri: 64.45 (FTG)	1130
PD13	M	60	52/24	Chest Ri	R17	13	10	25	Le: C+L3(4,5,6)- Ri: C+L2.5(9,10,11,12,13,14)-	Le: 2.5/60/125 Ri: 1.8/60/125	Le: L2(1,2,3)L4(7) Ri: L1(8)L4(15)	Le: 15.63 (B) Ri: 62.50 (FTG)	390
PD20	F	69	45/11	Chest Ri	R22	10	8	30	Le: C+L3(4,5,6)- Ri: C+L2(9,10,11)-	Le: 2.7/60/125 R: 2.6/60/125	Le: L2(1,2,3)L4(7) Ri: L1(8)L3(12–14)	L: 18.55 (B) R: 62.50 (FTG)	150
PD22	M	67	38/23	Chest Ri	R21	10	5	33	Le: C+L3(4,5,6)- Ri: C + L3(12,13,14)-	Le: 1.9/60/125 R: 1.7/60/125	Le: L2(1,2,3)L4(7) Ri: L2(9,10,11)L4(15)	Le: 22.46 (B) Ri: 62.50 (FTG)	350

Abbreviations: PID, patient identifier; Pre-Op, pre-operative; UPDRS, Unified Parkinson's disease rating scale Part III; IPG, implantable pulse generator; RID, recording identifier; y, years; m, months; d, days; A, amplitude; PW, pulse width; Fs, stimulation frequency; LEDD, levodopa equivalent daily dose; M, male; Le, left; C, case; L, level; Ri, right; LF, low-frequency activity; B, β activity; FTG, finely-tuned gamma activity; F, female.
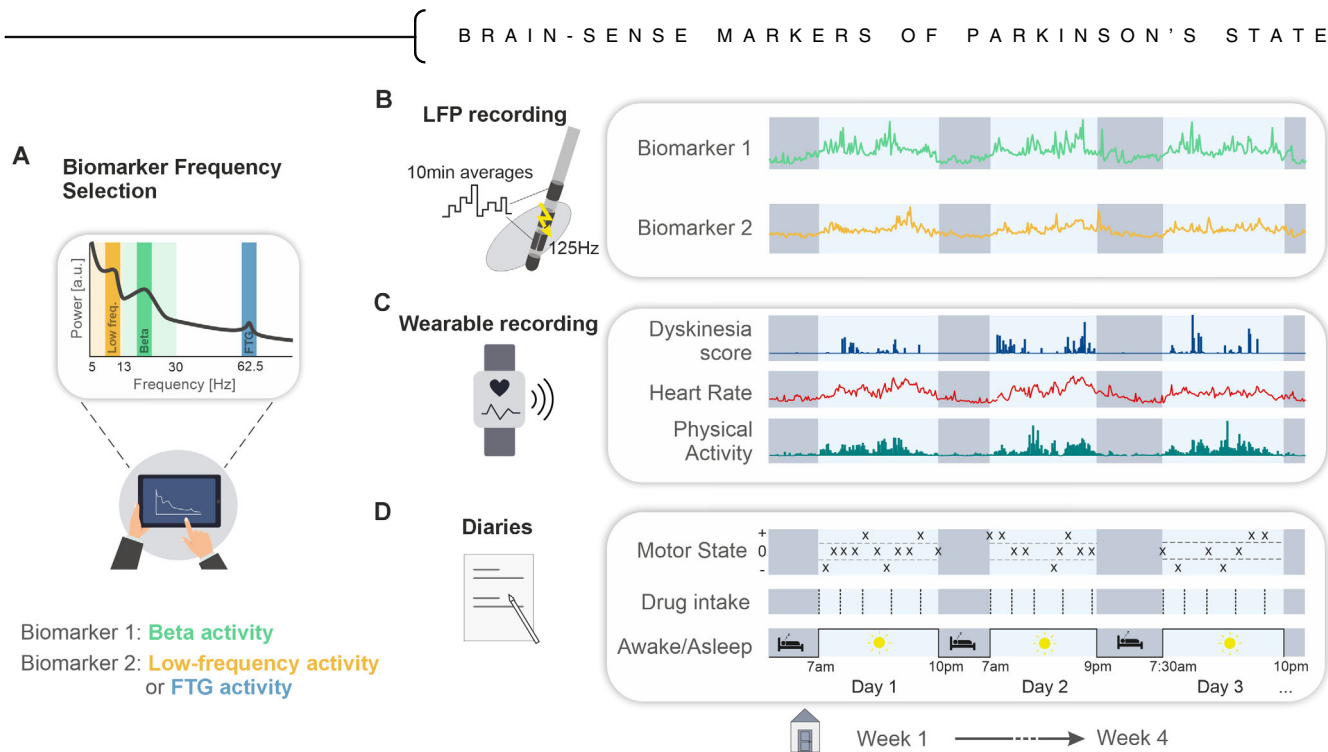
FIG. 1. Method figure: Ambulatory multimodal data recording. Schematic illustration of the experimental setup with the main parts of the multimodal assessment over 4 weeks per study period. (**A**) Biomarker frequency selection for each hemisphere separately after running the BrainSense Setup (Signal Check) on the Medtronic tablet. For biomarker 1, β activity is selected, whereas for biomarker 2, either low frequency or FTG activity at half the stimulation frequency is selected, alternating if a second recording period took place. (**B**) Bi-hemispheric registration of STN LFP of a preselected neurophysiological biomarker using the Percept BrainSense timeline feature of the sensing-enabled Medtronic Percept PC. An average power value is saved over every 10-minute time window. (**C**) Wearables were used for the collection of physical activity data, heart rate, and a dyskinesia score. (**D**) Paper-based diaries were used for self-assessment of the subjective motor state (+: dyskinetic, 0: optimal, −: akinetic), medication schedule, as well as wake-up and go-to-bed times. LFP: local field potentials; STN: subthalamic nucleus; FTG: finely tuned γ. [Color figure can be viewed at wileyonlinelibrary.com]

Wearable Recordings

Using the Food and Drug Administration (FDA)-cleared StrivePD application (Rune Labs, San Francisco, CA, USA), acceleration and heart rate data were passively recorded using an Apple Watch (Apple Inc., Cupertino, CA, USA) and transmitted to the cloud platform of Rune Labs (Fig. 1C). The percentage time of dyskinesia was determined by the Motor fluctuations Monitor for Parkinson's Disease (MM4PD) algorithm.[50] From recording R07 (PD07) onward, we additionally introduced the AX6 accelerometer (Axivity Ltd, UK) with a 4-week lasting battery life in order to reduce the recording gaps in the acceleration data (re-charging gaps from Apple Watch). To maximize the adherence, patients could freely choose the side to wear the wearables.

Symptom Diary and Sleep–Wake Times

Participants were instructed to document their subjective motor state in a paper-based (Fig. 1D) version of the PD home diary,[51] modified to allow a greater degree of motor states.[52] A score of 0 indicated an optimal motor state, 1 to 3 indicated mild to severe dyskinesia, and −1 to −3 indicated mild to severe akinesia (details, supplementary). To better track the circadian cycles, participants also reported daily time-to-bed and wake-up times.

Medication-Intake Events

Medication-intake events were defined around intakes of L-dopa formulation doses (L-dopa/Benserazide, L-dopa/Carbidopa) throughout the day. Patients were instructed to report timing and dosage of medication when deviating more than 30 minutes from their regular schedule. Prolonged release L-dopa formulations, dopamine agonists, or other PD medication were not considered in the analyses. The analysis window expanded up to 120 minutes after the intake to maximize the likelihood of capturing the *off*-to-*on* transition, whereas the period from 0 to 30 minutes was considered as baseline.

Multimodal Data Processing and Analysis

LFP and Apple Watch data were synchronized using the Rune Labs platform and then time-aligned to the AX6-acceleration data using custom MATLAB scripts. LFP data were screened and corrected for outliers using a previously published method.[48] Bio-signals and paper-based diaries were resampled to match the 10-minute average power interval of the LFP timeline series. Medication-intake times and asleep/awake times were assigned to the temporally nearest LFP data point. The transformation of acceleration data into physical activity was computed based on an established algorithm (see supplementary).[53] The processing steps of

the in-hospital LFPs are described in the supplementary. To assess circadian brain signal properties, recordings were divided into awake and asleep periods based on the information provided in the diaries. We compared mean LFP power and its standard deviation in the two states, reporting the percentage change from asleep to awake. The awake state was further divided into low and high activity periods by a median split, and the percentage change was calculated. To assess dopaminergic medication effects, LFP data were z-scored for each intake period, and the median was calculated across all intakes. The first and last daily intakes were compared to in-between intakes. The relationship between biomarkers and symptoms was based on z-scored and concatenated awake state LFP data. For the evaluation of objectively measured symptom scores, we correlated the normalized LFP power and the wearables data from each patient across all days. To account for dyskinesia's influence on LFP power during medication-intake windows, we calculated the ratio of LFP power to dyskinesia scores and excluded intakes with any self-reported positive dyskinesia scores post-intake.

Statistics

All statistical analysis was performed using *MATLAB* (version R2022b; The MathWorks Inc.). Normality of data distribution was assessed visually using QQ-plots. To compare LFP power between asleep/awake, low/high physical activity, and low/high heart rate states, the percentage change was tested for significance using the Wilcoxon signed-rank test. For multiple comparisons, *P*-values were FDR (false discovery rate) corrected.[54] Differences across biomarkers were assessed using the Kruskal-Wallis test. Post-hoc analysis for this test was performed using the *multcompare* function, employing Tukey's honestly significant difference procedure. Spearman partial correlation was computed between each biomarker and mean dyskinesia duration, as well as across biomarkers, controlling for physical activity and heart rate, with significance assessed using the Wilcoxon signed-rank test and FDR-corrected *P*-values. The effect of medication intakes on the biomarkers over time was analyzed using Friedman's test. Post-hoc analysis was performed using Dunnett's test, comparing each time point to the median of the baseline window.

Results

Multimodal neurobehavioral data were collected from 14 patients over 25 to 70 days. Three patients underwent 4-week recording periods with the β/low-frequency configuration, 3 with the β/FTG configuration, and 8 participated two 4-week recording periods

using both configurations (Fig. S2). The spectral curves and baseline characteristics for all patients are described in Tables S1, S2 and S3 and Figures S2–S6.

Influence of Circadian Rhythms and Confounding Factors

We first investigated the circadian rhythmicity of the three biomarkers (low-frequency activity, β activity, and FTG activity) (Fig. 2A). All biomarkers showed a significant increase in power during wakefulness compared to sleep (low-frequency: 17.9%, $P_{FDR} = 0.007$; β activity: 75.7%, $P_{FDR} < 0.001$; FTG: 48.5%, $P_{FDR} = 0.001$, Wilcoxon signed-rank test). The increase in β activity was significantly higher compared to the low-frequency activity, with no significant difference between the other biomarkers (Fig. 2B). We also compared the volatility of the biomarkers expressed as their change in standard deviation, which significantly increased from the sleep to the awake time (low-frequency: 70.8%, $P_{FDR} = 0.007$; β activity: 36.2%, $P_{FDR} = 0.001$; FTG: 57.6%, $P_{FDR} = 0.001$, Wilcoxon signed-rank test), without a significant difference between the biomarkers (Fig. 2C). The increasing trend in power and volatility was also observed at the individual level (Fig. S7A,B). Second, we evaluated the impact of physical activity and heart rate activity by dividing the awake-time LFP recordings into high and low activity and heart rate states based on median-splits (Fig. 2D). High physical activity states led to a power increase in all biomarkers compared to low activity states (low-frequency: 11.5%, $P_{FDR} = 0.005$; β: 14.4%, $P_{FDR} < 0.001$; FTG: 28.4%, $P_{FDR} = 0.001$, Wilcoxon signed-rank test). FTG power increased significantly more than low-frequency power, with no significant differences found in the other biomarkers (Fig. 2E). In contrast, controlled, in-hospital, high-resolution LFP assessments show a significant motion-related β desynchronization, whereas FTG and low-frequency activity behave the same as in the ambulatory recording (Fig. S8; Table S2). Periods of elevated heart rate also led to an increase in LFP power (low-frequency: 9.8%, $P_{FDR} = 0.007$; β: 19.6%, $P_{FDR} < 0.001$; FTG: 13.1%, $P_{FDR} = 0.001$; Wilcoxon signed-rank test), with no differences between biomarkers (Fig. 2F). These findings were also consistent and confirmed at the individual level (Fig. S7C,D). Additionally, the different biomarkers recorded in both hemispheres showed a significantly positive intercorrelation in their temporal dynamics during both asleep and awake periods (Fig. S9A), which remains preserved after correction for common confounding factors (Fig. S9B). Half of patients preferred the IPG implantation in the left instead of the recommended right-chest side. The related ECG-artifact detection was comparable (left:
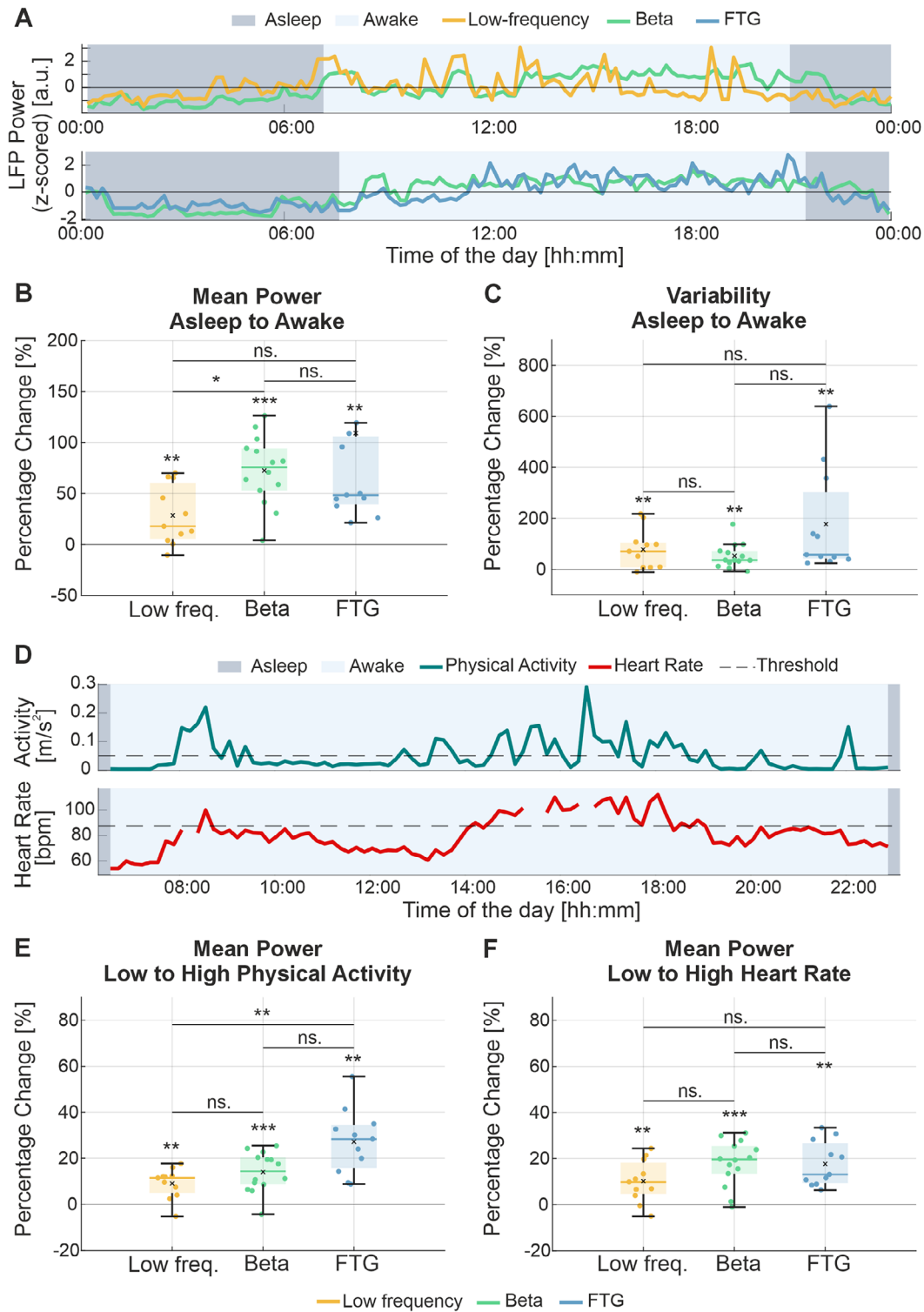
FIG. 2. Asleep/awake LFP power difference and effects of physical activity and heart rate. (**A**) Two entire days of asleep and awake fluctuations in biomarkers in different frequency bands of the left and right STN of a representative subject. (**B**) Shows the percentage change in the mean power of the awake state compared to the asleep state of all subjects for the three biomarkers (low-frequency activity: orange, β activity: green, FTG: blue). A positive value indicates a power increase during the awake compared to the asleep state. (**C**) Shows the change in power variability between the awake and asleep states of all subjects for the three biomarkers. A positive value indicates increased variability during awake compared to asleep. (**D**) Fluctuations in the physical activity state and the heart rate during 1 day. The dashed line presents the median within the full recording (awake states only) used to split the data into high and low activity and heart rate state, respectively. (**E**) Shows the percentage change in the mean power during high compared to low physical activity states of all subjects for the three biomarkers. A positive value indicates increased power during high compared to low activity state. (**F**) Shows the percentage change in mean power during high compared to low heart rate states of all subjects for the three biomarkers. A positive value indicates increased power during high compared to low heart rate. LFP, local field potentials; STN, subthalamic nucleus; FTG, finely tuned γ. [Color figure can be viewed at wileyonlinelibrary.com]

n = 7, 62.5%, right: n = 7, 55.6%), but more prominent on the left (Fig. S10).

Biomarkers Indexing Dopaminergic Medication States

A main goal of this work was to characterize the effects of the dopaminergic medication cycles on the dynamics of the three candidate biomarkers (Fig. 3A). After medication intake, FTG showed a power increase, reaching a statistical significance at 80 minutes and between 100 and 110 minutes (χ^2[12] = 34.99, $P < 0.001$, P_{Dunnet} (80, 100, 110) = [0.007, 0.015, 0.031], Friedman test) (Fig. 3B). In contrast, both low-frequency and β did not show a significant medication-related dynamic (Fig. 3B). Given the large circadian-dependent changes in LFP power (Fig. 2B,C), we investigated whether this affects the dynamics of medication intakes in proximity to day-night transitions. Thus, we split L-dopa-intakes into three daily intake groups: first, last, and in-between intakes. The first intake group showed an increasing trend across all biomarkers, whereas the last intake group showed a significant decreasing trend compared to in-between intakes (Fig. 3C). For the further analyses, we only focused on the in-between intakes. This resulted in an enlarged window (80–110 minutes) of significant medication-induced FTG increase (χ^2 [12] = 50.17, $P < 0.001$, P_{Dunnet} (80, 90, 100, 110) = [0.003, 0.001, 0.003, 0.007], Friedman test), whereas the other biomarkers remained uninformative (Fig. 3D). At the individual level, FTG activity significantly increased in 8 of 10 patients. In contrast, β increased in 5 of 14 patients, whereas low-frequency showed a significant increase in 2 of 10 and a decrease in 4 of 10 patients. The distribution of subjects with significant power changes per 10-minute window is shown in Figure 3D. These results were also preserved after correcting for confounding physical activity and heart rate (Fig. S11).

High-Resolution In-Hospital Recording to Inform Ambulatory LFP Dynamics

Here we aim to link the independently performed high-resolution in-hospital recordings with the low-resolution ambulatory recordings. Figure 4A illustrates the spectral curve dynamics of the cohort's in-hospital high-resolution recording in the four medication/stimulation conditions (time-frequency spectrograms are reported in Fig. S12). Of practical relevance in this context is the LFP dynamics following medication response while ON-stimulation captured in the ambulatory and in-hospital setting. We observed 40% of patients who decreased and 60% who increased their low-frequency activity, whereas 38% of patients decreased and 62% of

patients increased their β activity from *off* to *on* medication state. FTG showed a more consistent increase in 80% and decrease in 20% of patients (Fig. 4B), which indeed is most evident at half the stimulation frequency 62.5 Hz (Fig. S13). Note, repeating the same assessment, but with stimulation switched OFF, we see a significant power decrease in β activity. The same was true for the effect of stimulation while in the OFF-medication state (Fig. S14 and Table S3). The match for presence and direction of the LFP-response to medication between in-hospital and ambulatory settings was highest for FTG (89%), followed by β (67%) and low-frequency activity (40%) (Fig. 4C), whereas the magnitude of the response per se was not related (Fig. S13).

Ambulatory Biomarkers Indexing Symptom States

Finally, we investigated whether the biomarkers can index the motor symptom state or dyskinesia in the ambulatory setting. This revealed a positive significant correlation between the wearable-based dyskinesia score and FTG as well as low-frequency activity at the group level (low-frequency: $\rho = 0.07$, $P_{FDR} = 0.003$; FTG: $\rho = 0.06$, $P_{FDR} = 0.003$, Wilcoxon signed-rank test) (Fig. 5A). For this analysis, we have corrected both LFP activity and dyskinesia score for physical activity and heart rate, given the strong correlation (Fig. S15). At the subject level, a significant correlation was evident for FTG (6 of 11 patients with a significantly positive correlation), followed by β activity (5 of 13 with a significantly positive and 2 of 13 patients with a significantly negative correlation) and low-frequency activity (2 of 10 patients with a significantly positive correlation). The self-reported motor states were summarized into negative (−1, akinesia), neutral (0, balanced), and positive (+1, dyskinesia) to increase the robustness (Fig. S16). Here, we found that FTG activity was higher during periods of subjective dyskinetic states compared to subjective optimal states and significantly higher (χ^2[12] = 13.83, $P < 0.001$, $P_{Tukey} < 0.001$, Kruskal-Wallis test) than during akinetic states (Fig. 5B). No significant relationship was found for the other biomarkers (Fig. 5B). Finally, we re-tested the ability of the biomarkers to index medication states correcting for the influence of both, objectively measured and self-reported dyskinesia. This confirmed the significant increase of FTG 80–90 minute post-intake (χ^2[12] = 32.82, $P = 0.001$, P_{Dunnet} (80, 90) = [0.03, 0.02], Friedman's test), whereas no significant dynamic was revealed for the other biomarkers (Fig. 5C). These findings were also consistent at the individual level (Fig. S15).
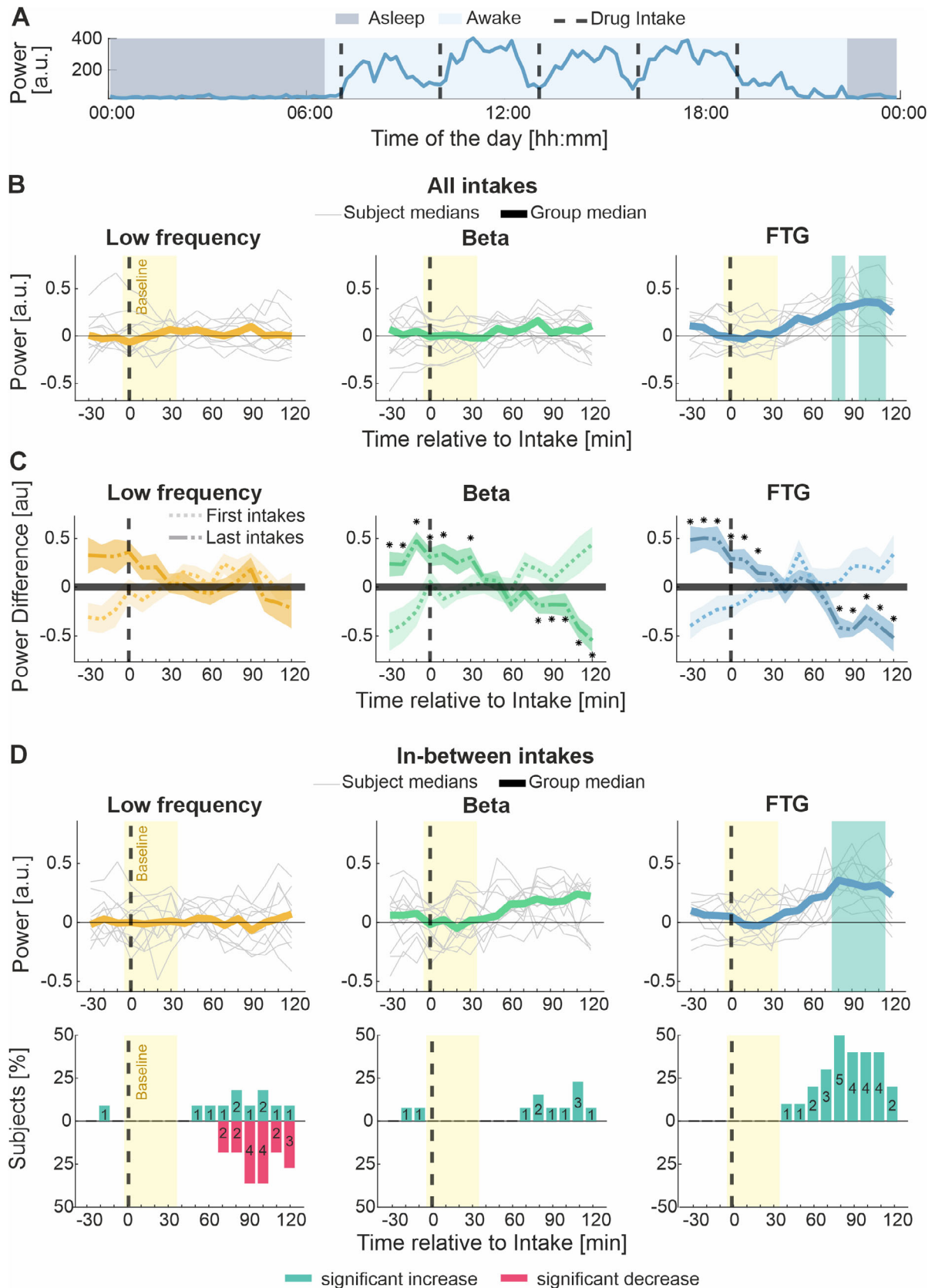
FIG. 3. Legend on next page.

Discussion

This work highlights the dynamics of three neurophysiological candidate symptom biomarkers (low frequency, β, and FTG activity) in PD patients implanted with a sensing-enabled neurostimulator over 25 to 70 days in real-life settings. We investigated the relationship to dopaminergic medication cycles, motor fluctuations, and circadian rhythmicity. Although subjects were on therapeutic stimulation and regular medication, FTG was the only biomarker that consistently fluctuated with the medication cycle. The presence of this dynamic could be anticipated from in-hospital high-resolution recordings. Both FTG and low-frequency activity correlated with the presence of dyskinesia. Importantly, FTG also indicated the ON-medication state regardless of the presence of dyskinesia. All biomarkers exhibited a strong circadian rhythmicity, as well as a power increase during periods of high movement and heart rate activity. Even after correcting for these confounding factors, FTG activity remained informative. This systematic neurobehavioral biomarker evaluation provides valuable insights into their long-term properties relevant for evolving sensing-guided therapies.

Biomarkers Indexing Medication Cycles and Symptom States

The era of aDBS is just beginning, and the ability to study neurophysiological biomarkers in patients' home environments marks a significant milestone. The primary goal of aDBS is to achieve an optimal balance between stimulation and medication effects for improved and personalized symptom control. We therefore selected three candidate biomarkers with prior evidence of being indicative of dopaminergic medication effects and symptom states and compared them in a real-life setting.[4] Starting with the medication states, we observed that FTG was the only biomarker to consistently exhibit dynamic fluctuations corresponding to the dopaminergic medication cycle, being low around the time of L-dopa-intake and increasing thereafter.[55] Notably, the dynamic response of FTG activity to medication was observed at group and subject levels and its presence, not its magnitude, can be anticipated from in-hospital high-resolution recordings. Importantly, although FTG entrained at half-stimulation frequency does not always show a visually prominent peak, subtle, yet distinct changes from adjacent frequencies can be present. This finding overall expands previous similar results showing the presence of cortical FTG after medication intake using an investigational device.[31] In contrast, low-frequency and β dynamics did not index medication states at the group level, although some subject-specific indicative trends were observed. FTG and low-frequency activity both positively correlated with wearable-based dyskinesia measures, whereas patient-reported OFF/ON motor states were only linked to FTG activity. It is important to emphasize that the term FTG often subsumes two phenomena. Olaru et al recently linked narrowband gamma activity at higher frequencies (65–80 Hz) to dyskinesia in the absence of chronic stimulation.[27] In the present study, patients were examined ON stimulation, and the correlation coefficients between dyskinesia and FTG measured at 62.5 Hz (half the stimulation frequency) were of lower magnitude. We suggest that FTG during chronic DBS, presumably entrained by stimulation, primarily indexes *on* medication states, regardless of the presence of dyskinesia. Thus, FTG might represent a continuum, which initially can constitute a physiological interaction with the pro-kinetic motor network,[56] to then eventually index dyskinesia in case the stimulation or dopaminergic drive increases. This raises the question whether FTG may differentiate the balanced ON-medication state from a dyskinetic state. Although it may seem surprising that β activity did not index medication or symptom states, contrasting with previous findings,[9,10,12,57,58] our findings should be interpreted in the context of ongoing continuous stimulation already suppressing pathological β activity and limiting its modulation along with medication as shown in the in-hospital assessment. In the context of adaptive DBS, this would be different as therapeutic suppression of β activity would indicate the neurostimulator to decrease stimulation allowing β activity to dynamically evolve

FIG. 3. Impact of dopaminergic medication intakes on LFP power dynamics. (**A**) Asleep and awake fluctuation in FTG power in the STN of a representative subject within 1 day. Vertical lines represent the times of medication intakes. (**B**) Illustrates median power dynamic of the single subjects (gray line) and the group median in bold from 30 minutes before to 120 minutes after the medication intake for the three biomarkers (low-frequency activity: orange, β activity: green, FTG: blue). The turquois shaded area indicates significant power changes compared to the baseline window (yellow shaded area, 0 to +30 minutes after medication intake). (**C**) Presents the median power dynamics at the first and last medication intakes of the day by contrasting them against the medication intakes in-between the first and the last daily intakes. The shaded area illustrates the standard error of the group median. Significant time points are denoted with an asterisk. Before the intake and during the baseline period β activity: P_{FDR} (−30, −20, −10, 0, 10, 30) = [0.03, 0.007, 0.005, 0.003, 0.008, 0.039]; FTG: P_{FDR} (−30, −20, −10, 0, 10, 20) = [0.01, 0.01, 0.01, 0.01, 0.01 0.04], whereas post-baseline β activity: P_{FDR} (80, 90, 100, 110, 120) = [0.034, 0.005, 0.012, 0.003, 0.003]; FTG: P_{FDR} (80, 90, 100, 110, 120) = [0.022, 0.01, 0.02, 0.013, 0.022], (Wilcoxon signed-rank test). (**D**) Illustrates median power dynamic of the single subjects (gray line) and the group median in bold from 30 minutes before to 120 minutes after the medication intake for the three biomarkers when only considering the medication intakes in-between the first and the last intakes of the day. The turquois shaded area indicates significant power changes compared to the baseline window. The bars below show the percentage of subjects showing a significant power change compared to baseline for each 10-minute window. Turquois indicates a significant power increase, whereas red indicates a significant power decrease. LFP, local field potential; STN, subthalamic nucleus; FTG, finely tuned γ. [Color figure can be viewed at wileyonlinelibrary.com]
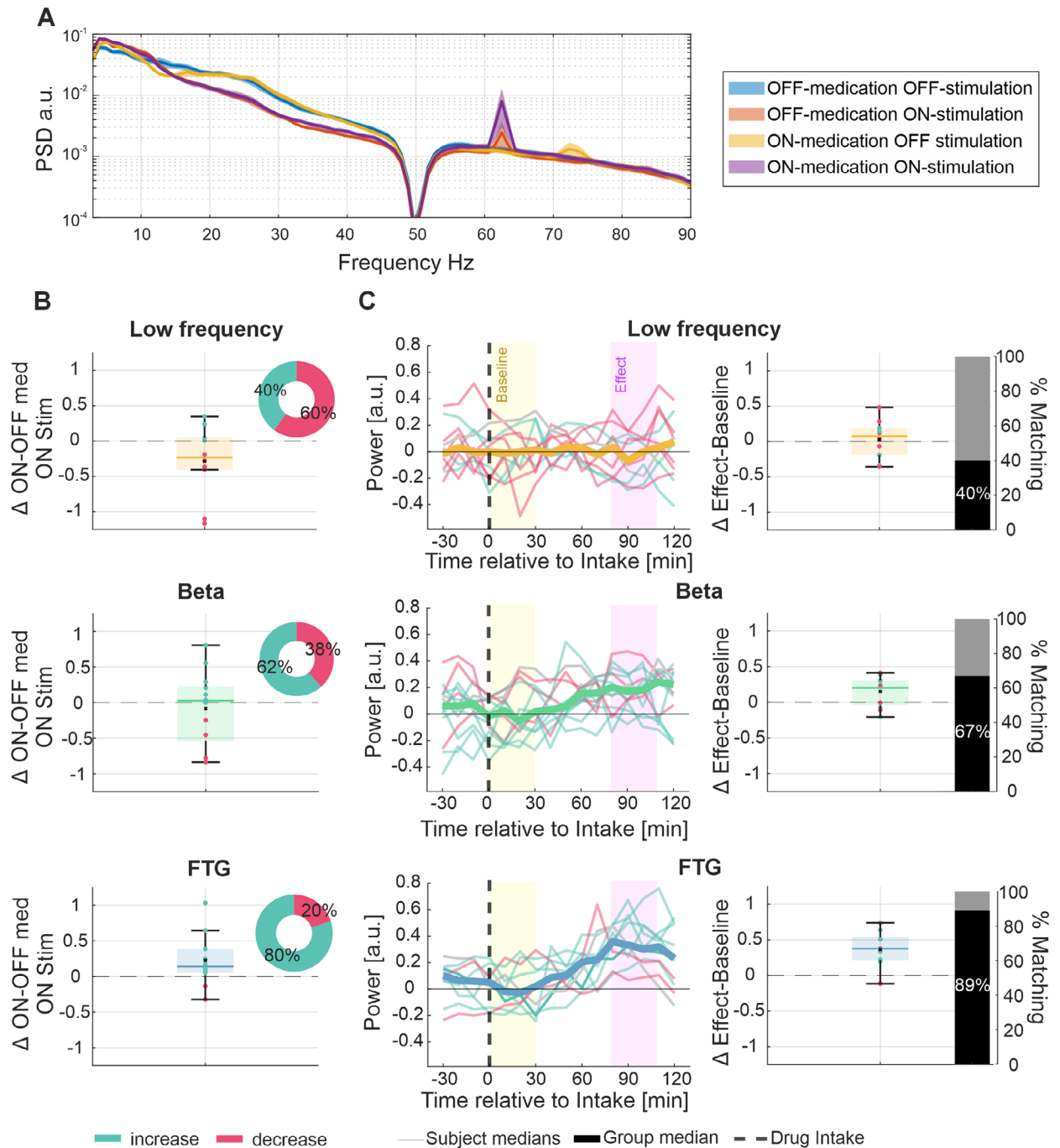
FIG. 4. Medication response in hospital and ambulatory recordings. (**A**) Group average spectra of the high-resolution LFP rest recordings (BrainSense Streaming mode) in the four medication/stimulation conditions. *off* medication/OFF stimulation (blue), *off* medication/ON stimulation (orange), *on* medication/OFF stimulation (yellow), and *on* medication/ON stimulation (violet). Medication alone preferentially reduces β band activity (most evident in 13–20 Hz), increases low-frequency activity (5–12 Hz), and induces FTG within 70–90 Hz. Stimulation alone reduces the β activity (13–30 Hz), increases low-frequency activity (5–12 Hz), and induces FTG at half the stimulation frequency (62.5 Hz, red curve). Combining stimulation and medication further amplifies stimulation-entrained FTG at 62.5 Hz (violet curve). (**B**) Illustrates the difference in LFP power for the three selected biomarker frequencies (low-frequency activity: orange, β activity: green, FTG: blue) between the medication *on* and *off* states (ON stimulation) measured in the hospital. Each dot represents a single subject. A positive value indicates a power increase from the *off* to the *on* medication state (turquois), whereas a negative value indicates a decrease (red). The pie chart shows the fraction of patients with an increase and decrease in the respective color. (**C**) Shows the effect of medication intake on the LFP power dynamic for the three selected biomarker frequencies in the ambulatory recording when considering only intakes between the first and last intakes of the day (Fig. 3C). On the right, the boxplot illustrates the difference between the mean power in the effect window (+80 to +110 minutes) and the baseline window (0 to +30 minutes). A positive value indicates a power increase in the effect window after medication intake, whereas a negative value indicates a decrease. Each line and dot represent a subject, and its color (red, turquois) is based on the result in (B). The gray line indicates the patient who did not participate in the in-hospital high-resolution recording. The bars present the percentage of patients (black) having the same trend in medication response in the hospital and in the ambulatory setting for the three biomarkers. LFP: local field potentials. FTG: finely tuned γ. [Color figure can be viewed at wileyonlinelibrary.com]
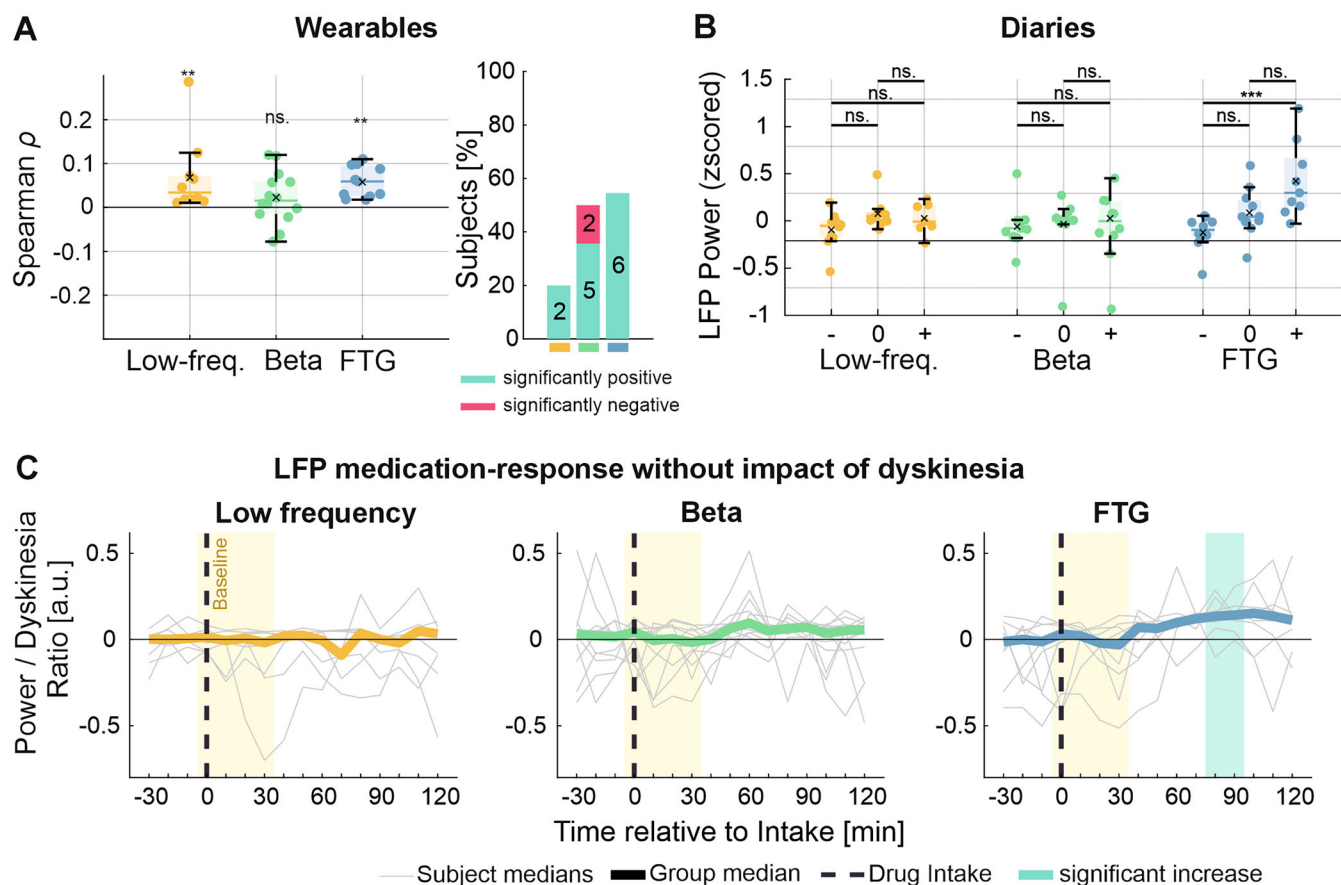
FIG. 5. Biomarkers indexing symptom states. (**A**) Shows the correlation between the dyskinesia score and the LFP power at the three selected biomarker frequencies (low-frequency: orange, β: green, FTG: blue) in the awake state within each subject. To correct for the influence of physical activity as well as for heart rate, partial correlation was applied. On the right, the bar plot indicates for each biomarker the percentage of subjects that had a significant correlation value. The color indicates whether a significant positive (turquois) or negative (red) correlation was observed. (**B**) Illustrates the mean LFP power of the three selected biomarker frequencies at the time points when the motor symptom state was marked in the symptom diaries. "0" represents an optimal motor state, whereas "−" indicates an akinetic state and "+" a dyskinetic state. (**C**) Illustrates the median ratio between the LFP power for the three biomarkers and the dyskinesia score when excluding the subgroup of intake windows with at least one self-reported positive dyskinesia score post-intake. Single subjects are reported in light gray and the group median in bold from 30 minutes before to 120 minutes after the medication intake. The turquois shaded area indicates significant changes in the ratio compared to the baseline window (yellow shaded area, 0 to +30 minutes after medication intake). LFP: local field potentials; FTG: finely tuned γ. [Color figure can be viewed at wileyonlinelibrary.com]

according to the respective control policy with its related stimulation amplitude configuration.[1,2,23,59]

Circadian Rhythmicity

The extended observational periods enable the assessment of longer temporal patterns, such as circadian rhythms.[8,25] All biomarkers, including low-frequency activity, display similar and intercorrelated circadian dynamics, with high power and volatility during wakefulness and reduced power at night. These dynamics may likely reflect intrinsic properties of the brain at different consciousness states, as these findings are preserved after controlling for artifacts from physical activity and heart rate, which expands on previous findings on this matter.[45,47,48] A critical observation for future aDBS designs is the substantial magnitude of power transitions between wakefulness and sleep that may mask the biomarker's medication-response dynamics during the first and last medication intakes of the

day. New dimensions of differentiated diurnal and nocturnal treatment modalities will likely be reached once devices allow for ambulatory high-resolution recordings that may allow us to differentiate sleep states and potentially sleep-related disorders from basal ganglia signals.[60-62]

Symptom Biomarker Susceptibility to Confounding Factors

Another relevant biomarker property to be evaluated is their susceptibility to confounding factors such as artifacts, considering the systems are miniaturized and implanted.[48,49,63] Our head-to-head comparison showed that all three biomarkers are similarly affected by heart rate activity as a direct consequence of the cardiac electrical field, which was more prominent for left-side-implanted neurostimulators.[64] Similarly, increased motion activity leads to confounding artifacts likely caused by associated hardware movement, also present

in all three biomarkers, which may for instance mask motion-related β synchronization. Interestingly, there might be a cause-effect dilemma for FTG as it can both increase due to motion artifacts and be biologically enhanced by voluntary motion and dyskinesia, as well as changing arousal states, making it challenging to further differentiate at the current state.

Clinical Implications and Sensing-Guided DBS

There are numerous ways how these candidate biomarkers could be embedded in aDBS algorithms.[65] Approaches evaluated in humans so far include suppressing pathological subcortical β activity, implemented through either single- or dual-threshold control at sub-second scales, or as slower proportional control at a 50 s time constant.[1,22,66] A distinct and successful approach utilizes cortical FTG processed over a ∼20–30 s time constant, which when elevated indexes stimulation to be reduced.[5,31] The feasibility of using subcortical low-frequency activity has been shown for dystonia, not yet for PD.[67] Based on the present results, we can derive the strongest conclusion in favor of using subcortical FTG as biomarker indexing *on*-medication states and therefore helping to balance stimulation based on medication fluctuations in an aDBS scenario. Yet, this control loop may be independent of the presence of dyskinesia, which is not in conflict with previous results from Olaru et al,[27] as the presence of FTG as suggested above represents a continuum.

Although these results are insightful, they also add to the complexity of parametrizing aDBS and the risk of overwhelming the present clinical routines. Hence effective approaches to quickly and accurately select biomarkers are needed. Both in-hospital and ambulatory assessment may contribute to such a clinical-neurophysiological interrogation strategy.[4,68] The intrinsic property of stimulation-entrained FTG, having its strongest signal-to-noise ratio at half the stimulation frequency, facilitates the biomarker selection. Yet, future studies could characterize the granularity of FTG dynamics in relationship to dyskinesia. In contrast, selecting the optimal biomarker frequency within the broader and functionally more heterogeneous low-frequency and β activity range may require a more refined approach with assessments at different medication doses and stimulation-intensity levels.[68] It also remains to understand whether the combined use of different biomarkers for both hemispheres can be additionally informative.

Limitations

Brain-sense signal recordings were continuous, but data from wearables and diaries may have been interrupted due to participants' compliance or technical limitations, that we aimed to compensate by a collection of representative data over multiple weeks. Interpretation of the data should overall be under consideration of the current technological limitation of low temporal resolution and restriction to a narrow spectral band of the ambulatory brain-sensing, that limits the interpretation on transient spectral state changes, and individual dynamics, and may be affected by broad band effects. It should be stressed that the experimental design performed exclusively under therapeutic stimulation may have favored the FTG properties. Furthermore, we did not always select the hemisphere with the most pronounced FTG for the ambulatory recording. A protocol conducted OFF or with subtherapeutic stimulation could have better evidenced the β dynamics related to medication and symptom states.

Conclusions and Outlook

This study presents a first head-to-head comparison of candidate biomarkers for aDBS using commercially available neurostimulator and DBS leads showing that FTG is the most powerful biomarker to index medication cycles at the group and individual levels. Yet, the field is at the beginning, and in the future, large-sample size and high-resolution ambulatory recordings will shed more light into more granular biomarker properties to advance the design and practical implementation of aDBS. ■

Data Availability Statement

Neural and wearable data can be made available upon request.

References

1. Little S, Pogosyan A, Neal S, et al. Adaptive deep brain stimulation in advanced Parkinson disease. Ann Neurol 2013;74(3):449–457. https://doi.org/10.1002/ana.23951

2. Arlotti M, Marceglia S, Foffani G, et al. Eight-hours adaptive deep brain stimulation in patients with Parkinson disease. Neurology 2018;90(11):e971–e976. https://doi.org/10.1212/WNL.0000000000005121

3. Bronte-Stewart H, Beudel M, Ostrem JLA, et al. Adaptive DBS algorithm for personalized therapy in Parkinson's disease: ADAPT-PD clinical trial methodology and early data (P1-11.002). Neurology 2023;100(17_supplement_2):3204. https://doi.org/10.1212/wnl.0000000000203099

4. Neumann WJ, Gilron R, Little S, Tinkhauser G. Adaptive deep brain stimulation: from experimental evidence toward practical implementation. Mov Disord 2023;38(6):937–948. https://doi.org/10.1002/mds.29415

5. Swann NC, De Hemptinne C, Thompson MC, et al. Adaptive deep brain stimulation for Parkinson's disease using motor cortex sensing. J Neural Eng 2018;15(4):46006. https://doi.org/10.1088/1741-2552/aabc9b

6. Groppa S, Gonzalez-Escamilla G, Tinkhauser G, et al. Perspectives of implementation of closed-loop deep brain stimulation: from neurological to psychiatric disorders. Stereotactic Funct Neurosurg 2023;102(1):40–54. https://doi.org/10.1159/000535114

7. di Biase L, Tinkhauser G, Martin Moraud E, Caminiti ML, Pecoraro PM, Di Lazzaro V. Adaptive, personalized closed-loop therapy for Parkinson's disease: biochemical, neurophysiological, and wearable sensing systems. Expert Rev Neurother 2021;21(12):1371–1388. https://doi.org/10.1080/14737175.2021.2000392

8. Tinkhauser G, Moraud EM. Controlling clinical states governed by different temporal dynamics with closed-loop deep brain stimulation: a principled framework. Front Neurosci 2021;15:734186. https://doi.org/10.3389/fnins.2021.73418615

9. Brown P, Oliviero A, Mazzone P, Insola A, Tonali P, Di Lazzaro V. Dopamine dependency of oscillations between subthalamic nucleus and pallidum in Parkinson's disease. J Neurosci 2001;21(3):1033–1038. https://doi.org/10.1523/jneurosci.21-03-01033.2001

10. Priori A, Foffani G, Pesenti A, et al. Rhythm-specific pharmacological modulation of subthalamic activity in Parkinson's disease. Exp Neurol 2004;189(2):369–379. https://doi.org/10.1016/j.expneurol.2004.06.001

11. Alonso-Frech F, Zamarbide I, Alegre M. Slow oscillatory activity and levodopa-induced dyskinesias in Parkinson's disease. Brain 2006;129(7):1748–1757. https://doi.org/10.1093/brain/awl103

12. Kühn AA, Kupsch A, Schneider GH, Brown P. Reduction in subthalamic 8-35 Hz oscillatory activity correlates with clinical improvement in Parkinson's disease. Eur J Neurosci 2006;23(7):1956–1960. https://doi.org/10.1111/j.1460-9568.2006.04717.x

13. Trottenberg T, Fogelson N, Kühn AA, Kivi A, Kupsch A, Schneider G-H, Brown P. Subthalamic gamma activity in patients with Parkinson's disease. Exp Neurol 2006;200(1):56–65. https://doi.org/10.1016/j.expneurol.2006.01.012

14. Neumann WJ, Degen K, Schneider GH, et al. Subthalamic synchronized oscillatory activity correlates with motor impairment in patients with Parkinson's disease. Mov Disord 2016;31(11):1748–1751. https://doi.org/10.1002/mds.26759

15. Tinkhauser G, Pogosyan A, Tan H, Herz DM, Kühn AA, Brown P. Beta burst dynamics in Parkinson's disease off and on dopaminergic medication. Brain 2017;140(11):2968–2981. https://doi.org/10.1093/brain/awx252

16. Tinkhauser G, Torrecillos F, Pogosyan A, et al. The cumulative effect of transient synchrony states on motor performance in Parkinson's disease. J Neurosci 2020;40(7):1571–1580. https://doi.org/10.1523/JNEUROSCI.1975-19.2019

17. Averna A, Debove I, Nowacki A, et al. Spectral topography of the subthalamic nucleus to inform next-generation deep brain stimulation. Mov Disord 2023;38(5):818–830. https://doi.org/10.1002/mds.29381

18. Neumann WJ, Turner RS, Blankertz B, Mitchell T, Kühn AA, Richardson RM. Toward electrophysiology-based intelligent adaptive deep brain stimulation for movement disorders. Neurotherapeutics 2019;16(1):105–118. https://doi.org/10.1007/s13311-018-00705-0

19. van Wijk BCM, de Bie RMA, Beudel M. A systematic review of local field potential physiomarkers in Parkinson's disease: from clinical correlations to adaptive deep brain stimulation algorithms. J Neurol 2023;270(2):1162–1177. https://doi.org/10.1007/s00415-022-11388-1

20. Eusebio A, Thevathasan W, Doyle Gaynor L, et al. Deep brain stimulation can suppress pathological synchronisation in parkinsonian patients. J Neurol Neurosurg Psychiatry 2010;82(5):569–573. https://doi.org/10.1136/jnnp.2010.217489

21. Trager MH, Koop MM, Velisar A, et al. Subthalamic beta oscillations are attenuated after withdrawal of chronic high frequency neurostimulation in Parkinson's disease. Neurobiol Dis 2016;96:22–30. https://doi.org/10.1016/j.nbd.2016.08.003

22. Velisar A, Syrkin-Nikolau J, Blumenfeld Z, Trager MH, Afzal MF, Prabhakar V, Bronte-Stewart H. Dual threshold neural closed loop deep brain stimulation in Parkinson disease patients. Brain Stimul 2019;12(4):868–876. https://doi.org/10.1016/j.brs.2019.02.020

23. Rosa M, Arlotti M, Marceglia S, et al. Adaptive deep brain stimulation controls levodopa-induced side effects in Parkinsonian patients. Mov Disord 2017;32(4):628–629. https://doi.org/10.1002/mds.26953

24. Swann NC, De Hemptinne C, Miocinovic S, et al. Gamma oscillations in the hyperkinetic state detected with chronic human brain recordings in parkinson's disease. J Neurosci 2016;36(24):6445–6458. https://doi.org/10.1523/JNEUROSCI.1128-16.2016

25. Gilron R, Little S, Wilt R, Perrone R, Anso J, Starr PA. Sleep-aware adaptive deep brain stimulation control: chronic use at home with dual independent linear discriminate detectors. Front Neurosci 2021;15:732499. https://doi.org/10.3389/fnins.2021.732499

26. Wiest C, Torrecillos F, Tinkhauser G, Pogosyan A, Morgante F, Pereira EA, Tan H. Finely-tuned gamma oscillations: spectral characteristics and links to dyskinesia. Exp Neurol 2022;351:113999. https://doi.org/10.1016/j.expneurol.2022.113999

27. Olaru M, Cernera S, Hahn A, et al. Motor network gamma oscillations in chronic home recordings predict dyskinesia in Parkinson's disease. Brain 2024;147(6):2038–2052. https://doi.org/10.1093/brain/awae004

28. Sermon JJ, Olaru M, Ansó J, et al. Sub-harmonic entrainment of cortical gamma oscillations to deep brain stimulation in Parkinson's disease: model based predictions and validation in three human subjects. Brain Stimul 2023;16(5):1412–1424. https://doi.org/10.1016/j.brs.2023.08.026

29. Duchet B, Sermon JJ, Weerasinghe G, Denison T, Bogacz R. How to entrain a selected neuronal rhythm but not others: open-loop dithered brain stimulation for selective entrainment. J Neural Eng 2023;20(2):26003. https://doi.org/10.1088/1741-2552/acbc4a

30. Mathiopoulou V, Habets J, Feldmann LK, et al. DBS-induced gamma entrainment as a new biomarker for motor improvement with neuromodulation. medRxiv 2024. https://doi.org/10.1101/2024.04.25.24306357v1

31. Oehrn CR, Cernera S, Hammer LH, et al. Chronic adaptive deep brain stimulation versus conventional stimulation in Parkinson's disease: a blinded randomized feasibility trial. Nat Med 2024;30(11):3345–3356. https://doi.org/10.1038/s41591-024-03196-z

32. Wiest C, Tinkhauser G, Pogosyan A, et al. Subthalamic deep brain stimulation induces finely-tuned gamma oscillations in the absence of levodopa. Neurobiol Dis 2021;152:105287. https://doi.org/10.1016/j.nbd.2021.105287

33. Manuel Alegre MDP, Lopez-Azcarate J, Fernando Alonso-Frech MD, Maria C, Rodrıguez-Oroz MDP, et al. Subthalamic activity during diphasic Dyskinesias in Parkinson's disease. Mov Disord 2012;27(9):1164–1168.

34. Wanga S, Chenb Y, Dingb M, et al. Revealing the dynamic causal interdependence between neural and muscular signals in Parkinsonian tremor. J Franklin Inst 2007;344:180–195.

35. Reck C, Florin E, Wojtecki L, et al. Characterisation of tremor-associated local field potentials in the subthalamic nucleus in Parkinson's disease. Eur J Neurosci 2009;29(3):599–612. https://doi.org/10.1111/j.1460-9568.2008.06597.x

36. Tass P, Smirnov D, Karavaev A, et al. The causal relationship between subcortical local field potential oscillations and parkinsonian resting tremor. J Neural Eng 2010;7(1):016009. https://doi.org/10.1088/1741-2560/7/1/016009

37. Shah SA, Tinkhauser G, Chen CC, Little S, Brown P. Parkinsonian tremor detection from subthalamic nucleus local field potentials for closed-loop deep brain stimulation. Annu Int Conf IEEE Eng Med Biol Soc 2018;2018:2320–2324. https://doi.org/10.1109/EMBC.2018.8512741

38. Asch N, Herschman Y, Maoz RCR, et al. Independently together: subthalamic theta and beta opposite roles in predicting Parkinson's tremor. Brain Commun 2020;2(2):fcaa074. https://doi.org/10.1093/braincomms/fcaa074

39. Sayfulina K, Filyushkina V, Usova SA, Gamaleya A, Tomskiy E, Belova A. Sedov periodic and aperiodic components of subthalamic nucleus activity reflect different aspects of motor impairment in Parkinson's disease. Eur J Neurosci 2025;61(1):e16648. https://doi.org/10.1111/ejn.16648

40. Nie Y, Luo H, Li X, Geng X, Green AL, Aziz TZ, Wang S. Subthalamic dynamic neural states correlate with motor symptoms in Parkinson's disease. Clin Neurophysiol 2021;132(11):2789–2797. https://doi.org/10.1016/j.clinph.2021.07.022

41. Ricciardi L, Fischer P, Mostofi A, et al. Neurophysiological correlates of trait impulsivity in Parkinson's disease. Mov Disord 2021;36(9):2126–2135. https://doi.org/10.1002/mds.28625

42. Bernasconi E, Amstutz D, Averna A, et al. Neurophysiological gradient in the Parkinsonian subthalamic nucleus as a marker for motor symptoms and apathy. npj Parkinsons Dis 2025;11(1):4. https://doi.org/10.1038/s41531-024-00848-2

43. Ricciardi L, Apps M, Little S. Uncovering the neurophysiology of mood, motivation and behavioral symptoms in Parkinson's disease through intracranial recordings. npj Parkinsons Dis. 2023;9(1):136. https://doi.org/10.1038/s41531-023-00567-0

44. Rodriguez-Oroz MC, López-Azcárate J, Garcia-Garcia D, et al. Involvement of the subthalamic nucleus in impulse control disorders associated with Parkinson's disease. Brain 2010;134(1):36–49. https://doi.org/10.1093/brain/awq301

45. Gilron R, Little S, Perrone R, et al. Long-term wireless streaming of neural recordings for circuit discovery and adaptive stimulation in individuals with Parkinson's disease. Nat Biotechnol 2021;39(9):1078–1085. https://doi.org/10.1038/s41587-021-00897-5

46. Balachandar A, Hashim Y, Vaou O, Fasano A. Automated sleep detection in movement disorders using deep brain stimulation and machine learning. Mov Disord 2024;39(11):2097–2102. https://doi.org/10.1002/mds.29987 2024

47. Cagle JN, de Araujo T, Johnson KAJ, et al. Chronic intracranial recordings in the globus pallidus reveal circadian rhythms in Parkinson's disease. Nat Commun 2024;15(1):4602. https://doi.org/10.1038/s41467-024-48732-0

48. van Rheede JJ, Feldmann LK, Busch JLJE, et al. Diurnal modulation of subthalamic beta oscillatory power in Parkinson's disease patients during deep brain stimulation. npj Parkinsons Dis. 2022;8(1):88. https://doi.org/10.1038/s41531-022-00350-7

49. Thenaisie Y, Palmisano C, Canessa A, et al. Towards adaptive deep brain stimulation: clinical and technical notes on a novel commercial device for chronic brain sensing. J Neural Eng 2021;18(4):42002. https://doi.org/10.1088/1741-2552/ac1d5b

50. Powers R, Etezadi-Amoli M, Arnold EMS, et al. Smartwatch inertial sensors continuously monitor real-world motor fluctuations in Parkinson's disease. Sci Transl Med 2021;13(579):eabd7865. https://doi.org/10.1126/scitranslmed.abd7865

51. Hauser RA, Deckers F, Lehert P. Parkinson's disease home diary: further validation amd implications for clinical trials. Mov Disord 2004;19(12):1409–1413. https://doi.org/10.1002/mds.20248

52. Löhle M, Bremer A, Gandor FJ, et al. Validation of the PD home diary for assessment of motor fluctuations in advanced Parkinson's disease. npj Parkinsons Dis 2022;8(1):69. https://doi.org/10.1038/s41531-022-00331-w

53. Doherty A, Jackson D, Hammerla N, et al. Large scale population assessment of physical activity using wrist worn accelerometers: the UK Biobank study. PLoS One 2017;12(2):e0169649. https://doi.org/10.1371/journal.pone.0169649

54. Benjamini YH. Controlling the false discovery rate - a practical and powerful approach to multiple testing. J R Stat Soc Ser B Stat Method 2012;57(1):289–300.

55. Hsu A, Yao HM, Gupta S, Modi NB. Comparison of the pharmacokinetics of an oral extended-release capsule formulation of carbidopa-levodopa (IPX066) with immediate-release carbidopa-levodopa (Sinemet®), sustained-release carbidopa-levodopa (Sinemet® CR), and carbidopa-levodopa-entacapone (.). J Clin Pharmacol 2015;55(9):995–1003. https://doi.org/10.1002/jcph.514

56. Muthuraman M, Bange M, Koirala N, et al. Cross-frequency coupling between gamma oscillations and deep brain stimulation frequency in Parkinson's disease. Brain 2020;143(11):3393–3407. https://doi.org/10.1093/BRAIN/AWAA297

57. Eusebio A, Brown P. Synchronisation in the beta frequency-band - the bad boy of parkinsonism or an innocent bystander? Exp Neurol 2009;217(1):1–3. https://doi.org/10.1016/j.expneurol.2009.02.003

58. Zaidel A, Spivak A, Grieb B, Bergman H, Israel Z. Subthalamic span of β oscillations predicts deep brain stimulation efficacy for patients with Parkinson's disease. Brain 2010;133(7):2007–2021. https://doi.org/10.1093/brain/awq144

59. Busch JL, Kaplan J, Habets JGV, et al. Single threshold adaptive deep brain stimulation in Parkinson's disease depends on parameter selection, movement state and controllability of subthalamic beta activity. Brain Stimul 2024;17(1):125–133. https://doi.org/10.1016/j.brs.2024.01.007

60. Urrestarazu E, Iriarte J, Alegre M, et al. Beta activity in the subthalamic nucleus during sleep in patients with Parkinson's disease. Mov Disord 2008;24(2):254–260. https://doi.org/10.1002/mds.22351

61. Thompson JA, Tekriwal A, Felsen G, et al. Sleep patterns in Parkinson's disease: direct recordings from the subthalamic nucleus. J Neurol Neurosurg Psychiatry 2017;89(1):95–104. https://doi.org/10.1136/jnnp-2017-316115

62. Zahed H, Zuzuarregui JRP, Gilron R, Denison T, Starr PA, Little S. The neurophysiology of sleep in Parkinson's disease. Mov Disord 2021;36(7):1526–1542. https://doi.org/10.1002/mds.28562

63. Ansó J, Benjaber M, Parks B, et al. Concurrent stimulation and sensing in bi-directional brain interfaces: a multi-site translational experience. J Neural Eng 2022;19(2):26025. https://doi.org/10.1088/1741-2552/ac59a3

64. Neumann WJ, Memarian Sorkhabi M, Benjaber M, et al. The sensitivity of ECG contamination to surgical implantation site in brain computer interfaces. Brain Stimul 2021;14(5):1301–1306. https://doi.org/10.1016/j.brs.2021.08.016

65. Guidetti M, Bocci T, De Pedro l Álamo M, et al. Adaptive deep brain stimulation in Parkinson's disease: a Delphi consensus study. medRxiv 2024. https://doi.org/10.1101/2024.08.26.24312580

66. Rosa M, Arlotti M, Ardolino G, et al. Adaptive deep brain stimulation in a freely moving parkinsonian patient. Mov Disord 2015;30(7):1003–1005. https://doi.org/10.1002/mds.26241

67. Piña-Fuentes D, van Zijl JC, Dijk JMC, et al. The characteristics of pallidal low-frequency and beta bursts could help implementing adaptive brain stimulation in the parkinsonian and dystonic internal globus pallidus. Neurobiol Dis 2019;121:47–57. https://doi.org/10.1016/j.nbd.2018.09.014

68. Alva L, Bernasconi E, Torrecillos F, et al. Clinical neurophysiological interrogation of motor slowing: a critical step towards tuning adaptive deep brain stimulation. Clin Neurophysiol 2023;152:43–56. https://doi.org/10.1016/j.clinph.2023.04.013

Supporting Data

Additional Supporting Information may be found in the online version of this article at the publisher's web-site.